LARGE EDDY SIMULATION OF AN OSCILLATING FLAME USING THE STOCHASTIC FIELDS METHOD

D. Fredrich[1], *W.P. Jones*[1] *and A.J. Marquis*[1]

[1] *Department of Mechanical Engineering, Imperial College London*

d.fredrich15@imperial.ac.uk

Abstract

Large eddy simulation (LES) of a partially premixed, swirl-stabilised flame is performed using a transported Probability Density Function approach solved by the stochastic fields method to account for turbulence-chemistry interaction on the sub-grid scales. The corresponding sub-grid stresses and scalar fluxes are modelled via a dynamic version of the Smagorinsky model and a gradient diffusion approximation, respectively. A 15-step reduced methane mechanism including 19 species is employed for the description of all chemical reactions. The test case involves a widely studied gas turbine model combustor with complex geometry and the simulation is carried out for a specific operating condition involving an oscillating flame. Overall, results of the velocity, temperature and major species mass fractions as well as the instantaneous thermochemical properties are shown to be in good agreement with experimental data, demonstrating the capabilities of the applied stochastic fields method. The inclusion of wall heat transfer in the combustion chamber is found to improve temperature predictions, especially in the near-wall regions. In summary, this work showcases the LES method's accuracy and robustness - none of the default model parameters are adjusted - for an application to complex, partially premixed combustion problems.

1 Introduction

The highly turbulent behaviour of swirl-stabilised flames involving fast chemical reactions and sophisticated geometrical features strongly limits our current understanding of the complex flow physics encountered in modern gas turbine combustors. A potentially powerful numerical tool capable of providing better insight into the physical processes associated with these turbulent reacting flows is large eddy simulation (LES). The concept behind LES methods is the direct computation of large-scale, energetic turbulent motions whereas the effects of motions whose 'size' is smaller than a defined filter width are modelled. One of the main challenges in the development of such methods for turbulent combustion is the interaction between turbulence and chemistry on the small, unresolved sub-grid (or subfilter) scales (*sgs*). These turbulence-chemistry interactions are governed by highly non-linear chemical reaction rates and appear in the form of a filtered source term in the LES scalar equations requiring extensive modelling work. Various combustion models addressing the closure problem have been proposed in the past, though most of them formulated for one specific burning regime only.

The sub-grid combustion model underlying the present work is based on a transported probability density function (PDF) approach solved by the fully Eulerian stochastic fields method. It has the advantage of a potentially regime independent description of turbulent flames, which becomes particularly useful in the context of gas turbine combustion. State of the art gas turbine combustors are designed to operate under lean, partially premixed conditions in order to effectively reduce pollutant emissions such as nitrogen oxides (NO_x) and carbon monoxide (CO). In the partially premixed flame regime, parts of the flow field are governed by premixed flame propagation and finite-rate effects, i.e. auto-ignition, extinction or ignition, while other parts will display mixing controlled reactions as encountered in diffusion (non-premixed) flames. It has been shown in the past, e.g. Jones and Navarro-Martinez (2007) and Jones and Prasad (2011), that it is possible to capture these phenomena within a single LES framework using the present stochastic fields method to account for turbulence-chemistry interaction. In a rigorous study of an industrial gas turbine combustor, Bulat et al. (2013) employed this LES formulation and achieved good reproduction of the experimentally measured flow statistics. Local extinction of the flame was shown to be due to turbulence-chemistry effects rather than large-scale mixing and the combustor was found to have regions in the diffusion flame regime.

A widely studied test case providing a solid basis for the validation of LES combustion models is the PRECCINSTA (Prediction and Control of Combustion Instabilities in Industrial Gas Turbines) burner. This gas turbine model combustor was experimentally investigated (e.g. Meier et al. (2007), Oberleithner et al. (2015), Yin et al. (2017)) and has been the focus of a number of computational simulations in the past (e.g. Roux et al. (2005), Moureau et al. (2011),

Wang et al. (2016), Fredrich et al. (2018), Gövert et al. (2018)). Comparisons between experiments and LES were first reported by Galpin et al. (2008) whose simulations predicted a higher burning rate - manifesting itself in a shortened flame length - and overestimated temperatures in the Outer Recirculation Zone (ORZ). The latter was attributed to the assumption of adiabatic combustion chamber walls, which preclude the replication of any wall heat transfer occurring in the experiments. These findings were later reinforced in ensuing LES studies by other authors coming to similar conclusions. Franzelli et al. (2012) underlined the importance of resolving the fuel injection, as opposed to prescribing a perfectly premixed mixture at the domain inlet, in order to obtain better agreement between the simulated and measured statistical quantities, especially in terms of root mean square (RMS) values. It has to be noted, that all of the above-cited numerical studies were performed using either simple chemistry involving very few species and reaction steps or tabulated chemistry based on fully premixed, laminar flame calculations.

In the present work, the flame regime independent stochastic fields method with reduced, yet comprehensive chemistry involving 15 steps and 19 species is applied to the PRECCINSTA model combustor including treatment of wall heat transfer. The objective is to evaluate the predictive capabilities of the employed LES method in the context of partially premixed combustion in a complex geometry. For this purpose, a specific combustor operating condition involving an oscillating flame is simulated and the results are compared against available measurement data; allowing for an assessment of the predicted flow field, flame topology, thermochemistry and major species concentrations - methane (CH_4) and carbon dioxide (CO_2) - as well as the influence of wall heat transfer.

2 Mathematical model

Filtered equations of motion

Applying a spatial, density weighted filter to the conservation equations of mass and momentum yields:

$$\frac{\partial \overline{\rho}}{\partial t} + \frac{\partial \overline{\rho}\widetilde{u}_i}{\partial x_i} = 0 \tag{1}$$

$$\frac{\partial \overline{\rho}\widetilde{u}_i}{\partial t} + \frac{\partial \overline{\rho}\widetilde{u}_i\widetilde{u}_j}{\partial x_j} = -\frac{\partial \overline{p}}{\partial x_i} + \frac{\partial}{\partial x_j}\left(2\mu\widetilde{S}_{ij}\right) - \frac{\partial}{\partial x_j}\tau_{ij}^{sgs} \tag{2}$$

The *sgs* stress tensor $\tau_{ij}^{sgs} = \overline{\rho}(\widetilde{u_i u_j} - \widetilde{u}_i\widetilde{u}_j)$ is evaluated via the dynamic version (Piomelli and Liu (1995)) of the Smagorinsky model $\mu_{sgs} = \overline{\rho}(C_s\Delta)^2(2\widetilde{S}_{ij}\widetilde{S}_{ij})^{1/2}$ where $\widetilde{S}_{ij}$ is the resolved strain tensor. The filter width Δ is taken to be the cube root of the local grid cell volume.

Sub-grid PDF evolution equation

In order to account for the influence of *sgs* contributions on the species formation rates, a joint *sgs* PDF, $\widetilde{P}_{sgs}$, is introduced representing the filtered product of the fine-grained PDF of each scalar - namely the reactive species and enthalpy. An exact equation describing the evolution of $\widetilde{P}_{sgs}$ can then be derived from the appropriate conservation equations using standard methods, e.g. Gao and O'Brien (1993). Taking into account the approach of Brauner et al. (2016) the modelled sub-grid PDF evolution equation becomes:

$$\begin{aligned}
&\overline{\rho}\frac{\partial \widetilde{P}_{sgs}(\underline{\psi})}{\partial t} + \sum_{\alpha=1}^{N_s}\sum_{\beta=1}^{N_s}\frac{\mu}{\sigma}\frac{\partial\widetilde{\phi}_\alpha}{\partial x_i}\frac{\partial\widetilde{\phi}_\beta}{\partial x_i}\frac{\partial^2\widetilde{P}_{sgs}(\underline{\psi})}{\partial\psi_\alpha\partial\psi_\beta} \\
&+\overline{\rho}\widetilde{u}_j\frac{\partial \widetilde{P}_{sgs}(\underline{\psi})}{\partial x_j} = \underbrace{-\sum_{\alpha=1}^{N_s}\frac{\partial}{\partial\psi_\alpha}\left[\overline{\rho}\dot{\omega}_\alpha(\underline{\psi})\widetilde{P}_{sgs}(\underline{\psi})\right]}_{\text{I: chemical reaction term (closed)}} \\
&\underbrace{+\frac{\partial}{\partial x_i}\left[\left(\frac{\mu}{\sigma}+\frac{\mu_{sgs}}{\sigma_{sgs}}\right)\frac{\partial\widetilde{P}_{sgs}(\underline{\psi})}{\partial x_i}\right]}_{\text{II: } sgs \text{ PDF transport term (gradient closure)}} \\
&\underbrace{-\frac{C_d}{2\tau_{sgs}}\sum_{\alpha=1}^{N_s}\frac{\partial}{\partial\psi_\alpha}\left[\overline{\rho}(\psi_\alpha-\widetilde{\phi}_\alpha(\mathbf{x},t))\widetilde{P}_{sgs}(\underline{\psi})\right]}_{\text{III: } sgs \text{ micro-mixing term (LMSE closure)}}
\end{aligned} \tag{3}$$

where ψ_α is the sample (or composition) space of each of the N_s scalars ϕ_α. The values 0.7 and 2.0 are assigned to the *sgs* Schmidt number σ_{sgs} and the *sgs* micro-mixing constant C_d, respectively. The *sgs* micro-mixing time scale is assumed to be given by $\tau_{sgs} = \overline{\rho}\Delta^2/(\mu_{sgs}+\mu)$. The right-hand side of Eq. (3) contains the chemical reaction term $\dot{\omega}_\alpha$ (I), which appears in closed form, as well as two additional unknown terms representing *sgs* transport of the PDF (II) and *sgs* micro-mixing (III). In the present work, these unknown terms are approximated, respectively, by a gradient closure directly analogous to the Smagorinsky model and by the linear mean square estimation (LMSE) closure (Dopazo and O'Brien (1974)).

Stochastic fields method

The closed form of the sub-grid PDF evolution equation is solved using the fully Eulerian stochastic fields method, where $\widetilde{P}_{sgs}(\underline{\psi})$ is represented by an ensemble of N stochastic fields $\xi_\alpha^n(\mathbf{x},t)$ for each scalar. In this work, the Itô formulation, as proposed by Valiño (1998), is adopted for the derivation of a system of stochastic differential equations equivalent to Eq. (3):

$$\begin{aligned}
\overline{\rho}\mathrm{d}\xi_\alpha^n + \overline{\rho}\widetilde{u}_i\frac{\partial\xi_\alpha^n}{\partial x_i}\mathrm{d}t = \\
\overline{\rho}\dot{\omega}_\alpha^n(\underline{\xi}^n)\mathrm{d}t + \frac{\partial}{\partial x_i}\left[\left(\frac{\mu}{\sigma}+\frac{\mu_{sgs}}{\sigma_{sgs}}\right)\frac{\partial\xi_\alpha^n}{\partial x_i}\right]\mathrm{d}t \\
-\frac{C_d\overline{\rho}}{2\tau_{sgs}}\left(\xi_\alpha^n-\widetilde{\phi}_\alpha\right)\mathrm{d}t + \left(2\overline{\rho}\frac{\mu_{sgs}}{\sigma_{sgs}}\right)^{1/2}\frac{\partial\xi_\alpha^n}{\partial x_i}\mathrm{d}W_i^n
\end{aligned} \tag{4}$$

Here, the Wiener process $\mathrm{d}W_i^n$ is approximated by time-step increments $\eta_i^n(\mathrm{d}t)^{1/2}$ where η_i^n is a $\{-1, 1\}$ dichotomic random vector, different for each field but independent of the spatial location $\mathbf{x}$. The filtered value of each scalar is obtained by averaging over the stochastic fields.

3 Test case

Experimental campaign

The well-known PRECCINSTA gas turbine model combustor considered in this work was initially the subject of an experimental test campaign conducted by Meier et al. (2007) at the DLR (German Aerospace Center). It involved a lean, partially premixed, swirl-stabilised, methane-air flame at atmospheric conditions with fuel injection taking place in a radial swirler. Flame oscillation caused by self-excited thermo-acoustic instabilities was observed at a global equivalence ratio of Φ_{glob} = 0.7. Relevant measurement uncertainties are presented in Table 1. These uncertainties are fairly low, hence allowing for a meaningful comparison of quantitative results between the experiment and LES.

Computational set-up

Figure 1 shows a vertical cut through the computational mesh. In order to account for preheating of the mixture, both air and methane are injected at a temperature of 320 K while the inflow pressure is set to 1 bar. The inlet velocities have been adjusted accordingly to reflect the prescribed mass flow rates. Isothermal wall temperatures are fixed at the combustion chamber side walls (1300 K) and base plate wall (700 K) based on experimental measurements by Yin et al. (2017). All other walls are treated as adiabatic with no-slip conditions. Radiative heat transfer is included in the simulations through the radiation model described in Barlow et al. (2001). A 15-step CH_4 mechanism with 19 species by Sung et al. (2001) is used to represent the chemistry. The in-house, block-structured, boundary conforming coordinate LES code BOFFIN-LES is employed to carry out the computation. It utilises a second-order-accurate finite volume method, based on a low-Mach-number, pressure based, variable density

Table 1: Systematic and statistical measurement uncertainties.

Measured quantity	Syst. uncertainty	Stat. uncertainty
Axial location h	±0.5 mm	
Radial location r	±0.5 mm	
Velocity	<0.5%	±1.5-2%
Temperature	±3-4%	±2.5%
Mixture fraction	±3-4%	±1%
CH_4 mole fraction	+5-9%	±1-3%
CO_2 mole fraction	±3-5%	±7%

Figure 1: Vertical cut through the generated mesh consisting of 2.7 million grid points distributed over 144 blocks.

formulation. None of the model's default parameters were adjusted for the simulation and eight stochastic fields are used to describe the influence of the sub-grid scale contributions.

4 Results and discussion

Flow field and flame topology

In order to visualise the flow field, Fig. 2 displays LES snapshots of the axial velocity, temperature and mixture fraction illustrating the highly turbulent flow and flame behaviour as well as the partially premixed nature of the combustor.

Radial profiles of the velocity at different downstream locations in the centre plane are presented in Fig. 3 allowing for a quantitative comparison between experiment and simulation. When characterising the flow field, three distinctive flow regions can be identified. An inner recirculation zone (IRZ), created by the swirling flow to stabilise the flame, can be easily detected due to the negative velocities around the combustor centreline. The conically shaped, swirling jet of unburnt gases is characterised by high axial velocities peaking at 40 m/s and high radial velocity magnitudes reaching approximately 20 m/s. Lower velocities to-

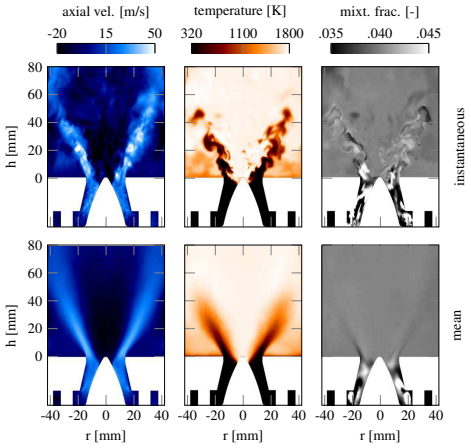

Figure 2: LES snapshots of the instantaneous (top) and mean (bottom) axial velocity, temperature and mixture fraction.

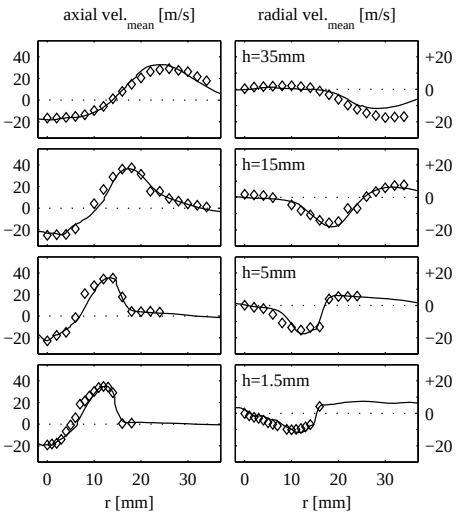

Figure 3: Radial profiles of the mean axial (left) and radial (right) velocity from the experiment (◊) and LES (—) - dotted line: zero velocity.

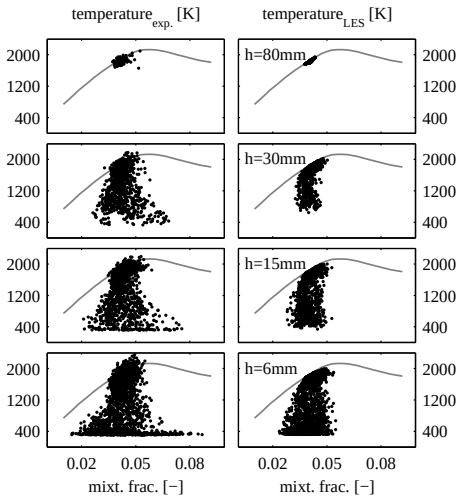

Figure 4: Experimental (left) and LES (right) scatter plots of the instantaneous temperature versus mixture fraction - solid line: adiabatic flame temperature.

wards the combustion chamber walls indicate the transition into an outer recirculation zone (ORZ), which is located outside of the experimentally measured region. With increasing downstream position, the high velocity jet widens and shifts towards the combustion chamber walls reducing the size of the ORZ while widening the IRZ. All of the above-mentioned flow characteristics are captured in the simulation and the quantitative velocity results match experimental data with very high accuracy.

Thermochemical properties

The predicted thermochemistry can be analysed in terms of the instantaneous relation between temperature and mixture fraction as depicted in Fig. 4. Looking at the evolution of the numerical temperature-mixture fraction distribution with downstream position, a shortened flame length can be determined corresponding to an overestimated burning rate. Compared to the experiment, the simulated temperatures approach the adiabatic flame temperature at a slightly quicker rate. Thus, at h = 15 mm for example, the simulated minimum temperatures are marginally higher compared to the experimental ones. This trend continues at h = 30 mm where all of the LES points have moved into either the reaction zone with intermediate temperatures or the fully burnt region, whereas the measurements still show a number of points remaining within the fresh gas region below ∼400 K. Finally, at h = 80 mm, both experimental and LES points are scattered exclusively around the adiabatic flame temperature indicating a fully burnt mixture.

In terms of the mixture fraction distributions, experimental extreme values of about 0.015 and 0.08 are observed; demonstrating that the premixing is indeed not perfect. The LES does not reproduce such a wide range of mixture fraction values but instead predicts a somewhat higher degree of premixing. Increased premixing tends to affect the burning rate, and may therefore be identified as a potential reason for the shortened flame length. The expanded experimental mixture fraction distribution is likely to be caused by the occurrence of thermo-acoustic instabilities periodically varying the amount of fuel in the mixture, as observed experimentally by Meier et al. (2007) and numerically by Franzelli et al. (2012). Note that the low-Mach-number solver applied in this work will not propagate acoustic waves, prohibiting the reproduction of thermo-acoustic instabilities. Nonetheless, the overall computed instantaneous temperature-mixture fraction correlation matches the experimental results including a reasonably estimated mixture fraction distribution.

A more detailed analysis of the thermochemistry at the first downstream location (h = 6 mm) is carried out based on Fig. 5. The lower temperature limit suggests that the assumed inlet temperature of 320 K recreates experimental preheating of the mixture. Marginal histograms of the temperature and mixture fraction divided into three different radial regions representing the IRZ, jet and ORZ are displayed on the horizontal and vertical axes, respectively. The locations of the temperature and mixture fraction peaks are in good agreement for all three regions while the experimental point distributions are slightly more spread out, which is to be expected. Burnt gases in the IRZ and ORZ are well captured by the LES as evidenced by the high temperatures and narrow range of mixture fraction values in these regions. Significantly higher levels of unmixedness are found in the jet of mostly fresh gases with low temperatures (r ≈ 10 - 16 mm) in both the experiment and simulation.

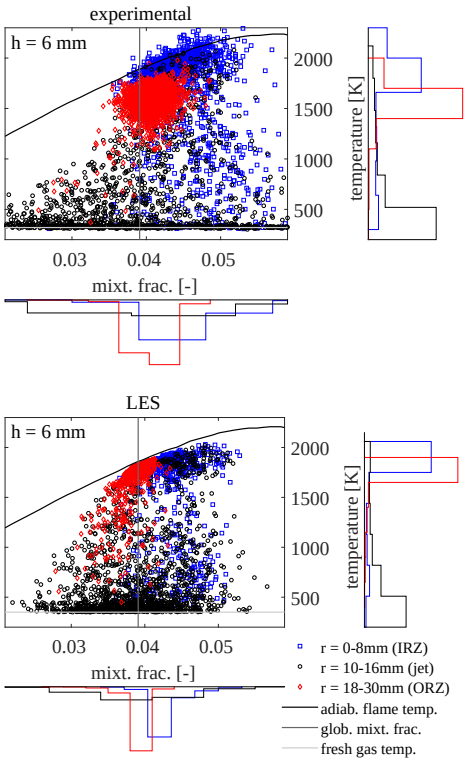

Figure 5: Instantaneous temperature-mixture fraction correlation from the experiment (top) and LES (bottom) at the first downstream location (h = 6 mm) including marginal histograms.

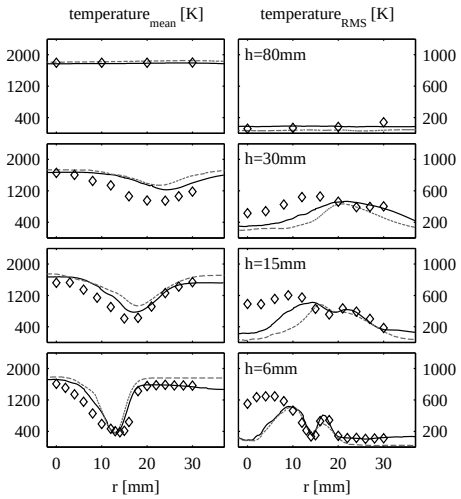

Figure 6: Radial profiles of the mean (left) and RMS (right) temperature from the experiment (◊), an LES with fully adiabatic walls (---) and the LES accounting for wall heat transfer (—).

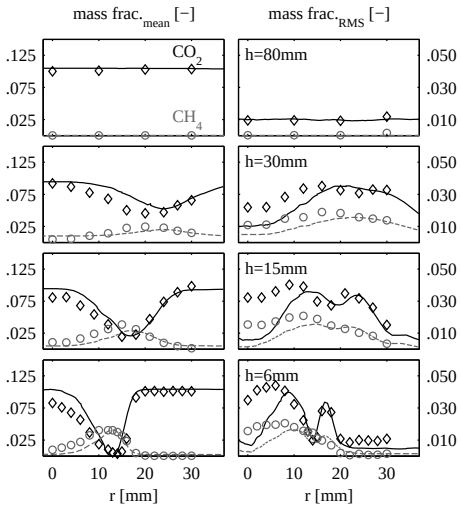

Figure 7: Radial profiles of the mean (left) and RMS (right) CO_2 and CH_4 mass fractions from the experiment (CO_2 ◊, CH_4 ○) and LES (CO_2 —, CH_4 ---).

Wall heat transfer and species concentrations

Figure 6 presents radial profiles of the temperature with and without wall heat transfer treatment. The general mean temperature trends including the location of the temperature dip representing unburnt gases are well reproduced by the LES. High temperatures near the centreline characterise the IRZ where burnt gases are transported back to the flame front with the purpose of stabilising the flame. By examining the mean and RMS temperature results of the two different LES cases, heat transfer can be identified as the source of local temperature overestimation towards the combustion chamber walls in the fully adiabatic LES. Overall, both the mean and RMS temperatures are in better agreement with measurements when wall heat transfer is included in the simulation.

Complementing the temperature results, radial profiles of the CO_2 and CH_4 mass fractions are shown in Fig. 7. A deviation between the measured and simulated temperature, CO_2 and CH_4 mass fraction profiles can be observed as a result of the under-predicted flame length first determined from Fig. 4. Hence, an earlier consumption of methane occurs leading to a local overestimation of CO_2. In accordance with the measurements, at h = 80 mm, the LES temperatures reach a homogeneous 'equilibrium' state around the adiabatic flame temperature of just over 1800 K and the methane is fully consumed.

From the RMS profiles depicted in Figs. 6 and 7 it becomes clear that the temperature, CO_2 and CH_4 mass fraction fluctuations are not sufficiently captured towards the combustor centreline. Again, the method's inability to reproduce thermo-acoustic instabilities serves as a potential explanation for the underestimation. In a previous LES of the same combustor, Franzelli et al. (2012) have shown an improvement of RMS temperature results close to the centreline by resolving thermo-acoustic instabilities using a fully compressible flow solver. Despite this shortcoming, RMS temperature profiles away from the centreline are accurately reproduced.

5 Conclusions

The PRECCINSTA gas turbine model combustor was successfully simulated using LES in conjunction with the stochastic fields method accounting for turbulence-chemistry interaction. The flow field was shown to be in excellent agreement with experimental data supporting the applicability of the solver with a dynamic sub-grid turbulence model to highly swirling flows. The mean temperature, CO_2 and CH_4 mass fraction profiles as well as the instantaneous thermo-chemical properties were generally well reproduced. A slightly under-predicted flame length corresponding to faster combustion was identified compared to experimental measurements. This was attributed to a somewhat overestimated degree of premixing potentially causing an increase in the burning rate. The inclusion of wall heat transfer was found to provide improved temperature results. Fluctuations of the temperature and major species mass fractions near the combustor centreline were not satisfactorily captured due to the flow solver's low-Mach-number formulation prohibiting any development of self-excited thermo-acoustic instabilities as observed in the experiments. A future extension of the solver to fully compressible flow will show if the unstable combustor behaviour can be reproduced. In summary, the predictive capabilities of the employed stochastic fields method have been demonstrated in the context of partially premixed combustion. All results were obtained without any adjustments to the default model parameters underlining the LES method's robustness and accuracy in the simulation of turbulent reacting flow problems in complex geometries.

Acknowledgments

The authors are grateful to SIEMENS Industrial Turbomachinery Ltd. for their financial support. This work was supported by the EPSRC through the UKCTRF and used the ARCHER UK National Supercomputing Service (`http://www.archer.ac.uk`).

References

Barlow, R.S., Karpetis, A.N., Frank, J.H. and Chen, J.Y. (2001), Scalar profiles and NO formation in laminar opposed-flow partially premixed methane/air flames, *Combust. Flame*, Vol. 127, pp. 2102-2118.

Brauner, T., Jones, W.P. and Marquis, A.J. (2016), LES of the Cambridge Stratified Swirl Burner using a Sub-grid pdf Approach, *Flow, Turbul. Combust.*, Vol. 96, pp. 965-985.

Bulat, G., Jones, W.P. and Marquis, A.J. (2013), Large Eddy Simulation of an industrial gas-turbine combustion chamber using the sub-grid PDF method, *Proc. Combust. Inst.*, Vol. 34, pp. 3155-3164.

Dopazo, C. and O'Brien, E.E. (1974), Functional formulation of nonisothermal turbulent reactive flows, *Phys. Fluids*, Vol. 17, pp. 1968-1975.

Franzelli, B., Riber, E., Gicquel, L.Y.M. and Poinsot, T. (2012), Large Eddy Simulation of combustion instabilities in a lean partially premixed swirled flame, *Combust. Flame*, Vol. 159, pp. 621-637.

Fredrich, D., Jones, W.P. and Marquis, A.J. (2018), Application of the Eulerian subgrid Probability Density Function method in the Large Eddy Simulation of a partially premixed swirl flame, *Combust. Sci. Technol.*, Advance online publication.

Galpin, J., Naudin, A., Vervisch, L., Angelberger, C., Colin, O. and Domingo, P. (2008), Large-eddy simulation of a fuel-lean premixed turbulent swirl-burner, *Combust. Flame*, Vol. 155, pp. 247-266.

Gao, F. and O'Brien, E.E. (1993), A large-eddy simulation scheme for turbulent reacting flows, *Phys. Fluids A*, Vol. 5, pp. 1282-1284.

Gövert, S., Mira, D., Kok, J.B.W., Vázquez, M. and Houzeaux, G. (2018), The Effect of Partial Premixing and Heat Loss on the Reacting Flow Field Prediction of a Swirl Stabilized Gas Turbine Model Combustor, *Flow, Turbul. Combust.*, Vol. 100, pp. 503-534.

Jones, W.P. and Navarro-Martinez, S. (2007), Large eddy simulation of autoignition with a subgrid probability density function method, *Combust. Flame*, Vol. 150, pp. 170-187.

Jones, W.P. and Prasad, V.N. (2011), LES-pdf simulation of a spark ignited turbulent methane jet, *Proc. Combust. Inst.*, Vol. 33, pp. 1355-1363.

Meier, W., Weigand, P., Duan, X.R. and Giezendanner-Thoben, R. (2007), Detailed characterization of the dynamics of thermoacoustic pulsations in a lean premixed swirl flame, *Combust. Flame*, Vol. 150, pp. 2-26.

Moureau, V., Domingo, P. and Vervisch, L. (2011), From Large-Eddy Simulation to Direct Numerical Simulation of a lean premixed swirl flame: Filtered laminar flame-PDF modeling, *Combust. Flame*, Vol. 158, pp. 1340-1357.

Oberleithner, K., Stöhr, M., Im, S.H., Arndt, C.M. and Steinberg, A.M. (2015), Formation and flame-induced suppression of the precessing vortex core in a swirl combustor: Experiments and linear stability analysis, *Combust. Flame*, Vol. 162, pp. 3100-3114.

Piomelli, U. and Liu, J. (1995), Large-eddy simulation of rotating channel flows using a localized dynamic model, *Phys. Fluids*, Vol. 7, pp. 839-848.

Roux, S., Lartigue, G., Poinsot, T., Meier, U. and Bérat, C. (2005), Studies of mean and unsteady flow in a swirled combustor using experiments, acoustic analysis, and large eddy simulations, *Combust. Flame*, Vol. 141, pp. 40-54.

Sung, C.J., Law, C.K. and Chen, J.-Y. (2001), Augmented reduced mechanisms for NO emission in methane oxidation, *Combust. Flame*, Vol. 125, pp. 906-919.

Valiño, L. (1998), A Field Monte Carlo formulation for calculating the probability density function of a single scalar in a turbulent flow, *Flow, Turbul. Combust.*, Vol. 60, pp. 157-172.

Wang, P., Fröhlich, J., Maas, U., He, Z. and Wang, C. (2016), A detailed comparison of two sub-grid scale combustion models via large eddy simulation of the PRECCINSTA gas turbine model combustor, *Combust. Flame*, Vol. 164, pp. 329-345.

Yin, Z., Nau, P. and Meier, W. (2017), Responses of combustor surface temperature to flame shape transitions in a turbulent bi-stable swirl flame, *Exp. Therm. Fluid Sci.*, Vol. 82, pp. 50-57.